

Fourier Transform Infrared Studies in Hypergolic Ignition of Ionic Liquids

Steven D. Chambreau,[†] Stefan Schneider,[†] Michael Rosander,[†] Tom Hawkins,[‡]
Christopher J. Gallegos,[‡] Matthew F. Pastewait,[‡] and Ghanshyam L. Vaghjiani^{*,‡}

Space and Missile Propulsion Division, Propulsion Directorate, Air Force Research Laboratory, AFRL/RZSP,
10 E Saturn Boulevard, Edwards AFB, California 93524

Received: April 28, 2008; Revised Manuscript Received: June 2, 2008

A class of room-temperature ionic liquids (RTILs) that exhibit hypergolic activity toward fuming nitric acid is reported. Fast ignition of dicyanamide ionic liquids when mixed with nitric acid is contrasted with the reactivity of the ionic liquid azides, which show high reactivity with nitric acid, but do not ignite. The reactivity of other potential salt fuels is assessed here. Rapid-scan, Fourier transform infrared (FTIR) spectroscopy of the preignition phase indicates the evolution of N₂O from both the dicyanamide and azide RTILs. Evidence for the evolution of CO₂ and isocyanic acid (HNCO) with similar temporal behavior to N₂O from reaction of the dicyanamide ionic liquids with nitric acid is presented. Evolution of HN₃ is detected from the azides. No evolution of HCN from the dicyanamide reactions was detected. From the FTIR observations, biuret reaction tests, and initial ab initio calculations, a mechanism is proposed for the formation of N₂O, CO₂, and HNCO from the dicyanamide reactions during preignition.

Introduction

There continues to be a growing effort to synthesize task-specific ionic liquids (ILs). Ionic liquids are salts with melting points below 100 °C. Lately, the design and choice of many ionic liquids is focused on physical properties such as miscibility, conductivity, viscosity, solubility, and melting points.¹ An interesting and important property of ionic liquids is that they have very low vapor pressures, with high heats of vaporization (approaching ~60 kcal mol⁻¹).² The details of how the chemical structure of the ionic liquid affects these various physical characteristics are now beginning to emerge.^{3–6} Less understood, but now of great interest, are the associated chemical properties that manifest in the condensed phase such as relative basicity (or acidity), oxidative (or reductive) capacity, thermal stability, electrochemical reactivity, and catalytic or combustion efficiency of the component ions.^{7–9}

Recent interest in room temperature ionic liquids has grown immensely, as their synthetic routes have been optimized. The number of publications involving ionic liquid chemistry has grown exponentially in the past decade.^{1,10,11} The number of possible different cation–anion combinations to form ILs is enormous, and so it is important to understand trends in reactivity and to have theoretical tools to screen for the best IL candidates for a given use. Typical cations for ionic liquids considered here include asymmetrically substituted imidazoliums and triazoliums, since symmetric cations tend to produce solid salts at room temperature.⁶ However, for a given cationic system, the choice of the anion is also important in tailoring the liquidus range of the salt.¹² Similarly, the chemical and thermal stabilities of the resulting IL can depend both on the physical (structural) and chemical properties of the individual component ions.^{9,13,14} For instance, in the case of imidazolium ionic liquids, studies have shown that the overall thermal stability of the IL correlates with the anion's size,¹⁵ its nucleophilicity (or its Lewis

basicity),^{13,16,17} and its hydrophilicity,¹⁸ etc. On the other hand, for a given anionic system, cationic size has little effect on the IL stability,^{18,19} while increased substitution of the imidazolium ring at the C(2)-site by straight-alkyl chains increases the stability but secondary or tertiary alkyl groups at the N-site decreases the stability.¹³

Recently, several groups have shown that some classes of ionic liquids can be distilled in a vacuum.²⁰ These ILs tend to have aprotic cations and non-nucleophilic anions, and studies have shown that the gas-phase species exist (in high vacuum) as neutral ion pairs and do not tend to vaporize as gas-phase clusters.^{21–23} For protic ionic liquids, however, the formation of neutral molecules in the gas phase has also been reported.²² An important thermochemical property which is difficult to obtain accurately for ionic liquids is the condensed phase heat of formation. Due to the ionic nature and liquid phase of ILs, theoretical calculations of the condensed phase heats of formation are difficult and have large uncertainties associated with them. Recent experimental measurements of heats of combustion and heats of vaporization of ILs have begun to accurately determine the condensed phase heat of formation for a few ionic liquids.^{24,25}

Here, we present the results of our efforts to tailor ionic liquids for utilization in bipropellant rocket engines. We desire not only to improve the performance (i.e., density specific impulse) over the current, state-of-the-art, monomethyl hydrazine/nitrogen tetroxide (MMH/NTO) system, but also be able to increase the ambient reactivity of the component ions toward common oxidizers, such that hypergolic ignition (spontaneous ignition upon mixing) is attained, comparable to MMH/NTO ignition times. To calculate performance characteristics of propellants, the condensed phase heat of formation value is critical.^{26,27} To successfully implement such ionic liquids into viable working systems, their physical properties such as viscosity and the liquid temperature range must also be tailored within required operational ranges.^{1,8} Furthermore, the inherent low vapor pressure of ionic liquids should significantly reduce the ambient toxicity and environmental emissions and therefore

* To whom correspondence should be addressed. E-mail: ghanshyam.vaghjiani@edwards.af.mil.

[†]ERC Inc.

[‡]Propellants Branch.

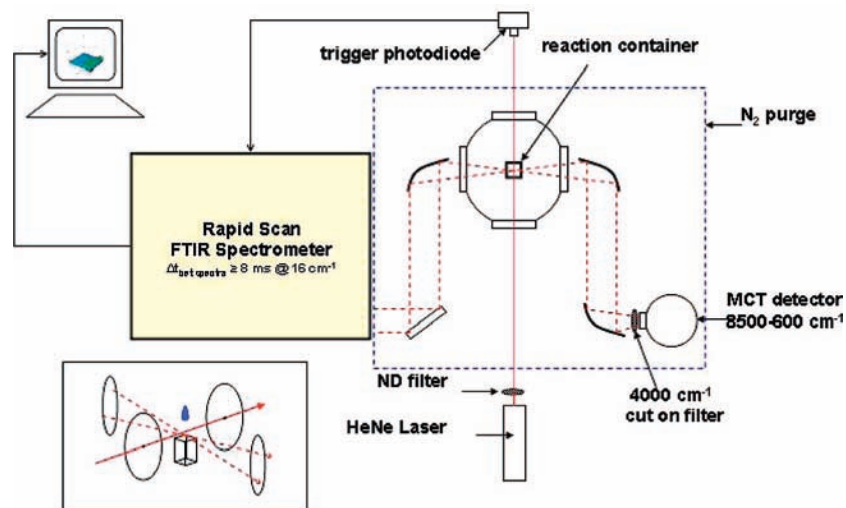


Figure 1. Schematic of the FTIR apparatus. The inset illustration in the lower left corner shows the relative positions of the HeNe laser beam, the IR beam, and the falling oxidizer droplet.

the associated cost of handling and fielding of these new replacement fuels. The extremely low vapor pressure of ionic liquids at ambient temperature and pressure is a major benefit of hypergolic ionic liquid fuels versus MMH, which is highly volatile. The high vapor toxicity of MMH increases the safety precautions required, and the logistics of handling it safely while loading the space-vehicle can be very expensive.

Understanding of chemical pathways and reaction mechanisms when fuels/ILs react with strong oxidizers is critical to designing new fuels. The current MMH/NTO hypergolic system has been used successfully for decades,^{28,29} and much theoretical work on the MMH/NTO system has been performed.^{30–35} However, little experimental work exists^{36–40} to confirm these results. Therefore, replacing the volatile, highly toxic, and carcinogenic MMH with a safer fuel is not a straightforward task. One of the challenges is that the mechanism involves highly reactive transient species which are difficult to probe experimentally.^{41,42} The identification of common reactive species in different hypergolic systems will play a significant role in future fuel design. There are two different regimes involved in hypergolic systems: first, the low-temperature preignition phase, where gaseous reactive species are produced and the temperature of the system increases as thermolytic and oxidative processes in the condensed phase begin to decompose both the fuel and the oxidizer. Once the temperature and concentrations of key species reach a critical level, ignition occurs in the gas phase,^{38,43} the temperature increases dramatically, and combustion occurs. To construct accurate numerical combustion models for IL hypergols, detailed chemical mechanistic information is needed on how fuel vaporization/pyrolysis processes compete with and augment concurrent and subsequent oxidative processes of the reactive fragments that are being produced.

Initial attempts by the Air Force Research Laboratory to design ILs with highly strained or unsaturated functional groups were made to introduce “trigger groups” onto the cation in the hope of inducing hypergolicity. These cations may be paired with oxygen-containing anions (NO_3^-) for oxygen balance or high heats of formation (N_3^-) to promote hypergolic ignition when treated with a suitable oxidizer.⁴⁴ The discovery that the anion can play a critical role in inducing hypergolicity is described here. The fact that a common anion can induce hypergolicity when paired with numerous different cations to form ionic liquids allows for the tailoring of the cation for

various desirable properties such as high heat of formation, low viscosity, a wide liquid temperature range, environmental safety, and thermal and shock stability. This paper describes the investigation of the preignition phase of hypergolic ignition of ionic liquids, a critical anion needed to induce hypergolic reactivity, and the influence of cation structure on the reactivity. This investigation focuses on white fuming nitric acid (WFNA) as the oxidizer.

Experimental Technique

Fourier-transform infrared (FTIR) absorption spectroscopy was performed using a rapid-scan spectrometer. Typical spectra were acquired in the range $590\text{--}3850\text{ cm}^{-1}$ with a spectral resolution of 2 cm^{-1} and approximately every 30 ms. The interferograms were recorded in split double-sided, split forward–backward mode. The reaction was carried out within a closed stainless steel chamber under constant nitrogen purge and therefore was carried out in an oxygen-free environment. Figure 1 shows the schematic of our experimental setup. The infrared beam was focused into the chamber above the reaction cell by means of gold mirrors and KRS-5 windows. A drop of oxidizer was introduced from a gastight syringe through a septum at the top of the chamber. The drop fell into a small cuvette containing a small amount ($0.1\text{--}1.0\text{ mL}$) of ionic liquid fuel. The spectrometer was triggered via a HeNe laser and photodiode positioned above the reaction cell. As the drop of oxidizer passes through the HeNe beam, the drop in signal from the photodiode triggers the spectrometer. Data was collected before the ignition flash occurs and is hereafter referred to as the preignition phase data.

To observe and measure the actual ignition delay (ID), a small fuel sample ($10\text{--}50\text{ }\mu\text{L}$) was instead dropped into the cuvette containing an excess amount (1.0 mL) of the oxidizer. A high-speed, complementary metal-oxide semiconductor (CMOS) video imager was used to record the time duration from the moment the fuel comes in contact with the liquid surface of the oxidizer and the first sign when a visible flame is formed, which invariably was always in the gas phase above the liquid surface. In the present work, the CMOS video settings of 1000 frames/sec and 168×512 pixel resolution were chosen. Figure 2 depicts typical observations for MMH/NTO, MMH/WFNA, and 1-propargyl-3-methyl-imidazolium dicyanamide/WFNA hypergolic ignitions for which the ID times were determined to

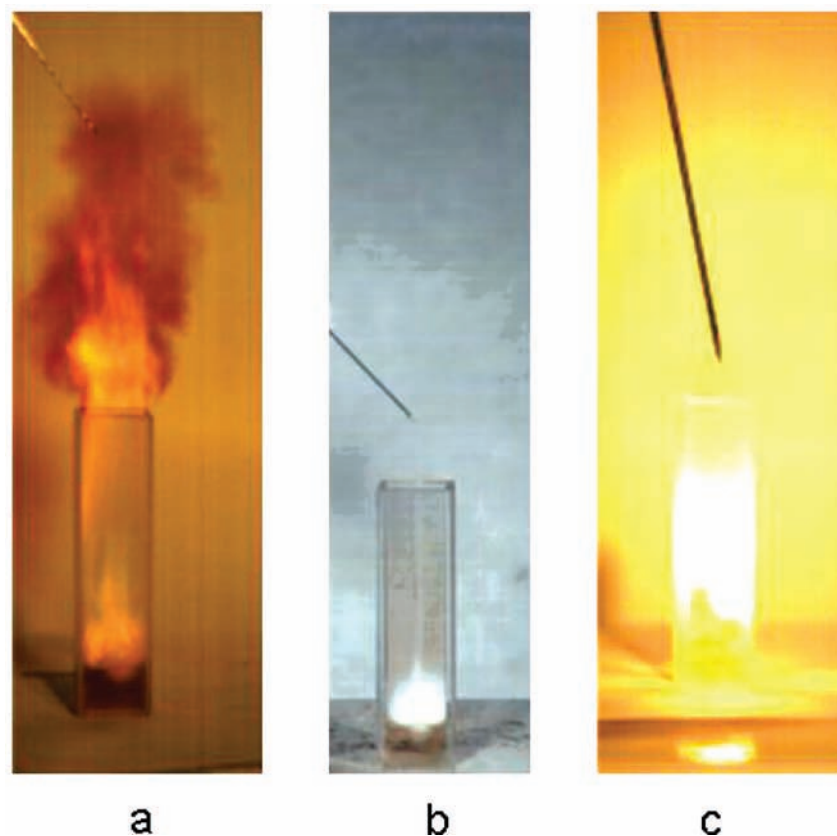


Figure 2. Hypergolic ignition of (a) MMH/NTO, ID = 1 ms; (b) MMH/WFNA, ID = 9 ms; and (c) 1-propargyl-3-methyl-imidazolium dicyanamide/WFNA, ID = 15 ms.

TABLE 1: Theoretical Reaction Enthalpies Calculated at the Hartree–Fock and Density Functional Theory Levels

reaction	ΔH_{0K} kcal/mol (zpe corrected)	method
$\text{NO}_3^- + \text{H}^+ \rightarrow \text{HNO}_3$	-318.5	B3-LYP 6-31G(+)(d,p)
$\text{N}(\text{CN})_2^- + \text{H}^+ \rightarrow \text{HN}(\text{CN})_2$	-302.8	B3-LYP 6-31G(+)(d,p)
$\text{N}(\text{CN})_2^- + \text{H}^+ \rightarrow (\text{NC})\text{N}(\text{CNH})$	-310.4	B3-LYP 6-31G(+)(d,p)
$\text{HN}(\text{CN})_2 + \text{H}^+ \rightarrow \text{H}_2\text{N}(\text{CN})_2^+$	-130.9	B3-LYP 6-31G(+)(d,p)
$(\text{NC})\text{N}(\text{CNH}) + \text{H}^+ \rightarrow (\text{NC})\text{NH}(\text{CNH})^+$	-166.2	B3-LYP 6-31G(+)(d,p)
$\text{N}(\text{NO}_2)_2^- + \text{H}^+ \rightarrow \text{HN}(\text{NO}_2)_2$	-303.8	RHF 6-31G(+)(d,p)
$\text{N}(\text{NO}_2)_2^- + \text{H}^+ \rightarrow \text{HN}(\text{NO}_2)_2$	-303.6	B3-LYP 6-31G(+)(d,p)
$\text{N}(\text{NO}_2)_2^- + \text{H}^+ \rightarrow (\text{O}_2\text{N})\text{N}(\text{NO}_2\text{H})$	-297.0	RHF 6-31G(+)(d,p)
$\text{HN}(\text{NO}_2)_2 + \text{H}^+ \rightarrow \text{H}_2\text{N}(\text{NO}_2)_2^+$	-169.9	B3-LYP 6-31G(+)(d,p)
$(\text{O}_2\text{N})\text{N}(\text{NO}_2\text{H}) + \text{H}^+ \rightarrow \text{H}_2\text{O} + \text{N}_2\text{O} + \text{NO}_2^+$	-212.4	RHF 6-31G(+)(d,p)
$\text{HN}(\text{NO}_2)_2 + \text{H}^+ \rightarrow \text{H}_2\text{O} + \text{N}_2\text{O} + \text{NO}_2^+$	-205.5	RHF 6-31G(+)(d,p)
$(\text{NC})\text{N}(\text{NO}_2)^- + \text{H}^+ \rightarrow (\text{NC})\text{NH}(\text{NO}_2)$	-307.8	RHF 6-31G(+)(d,p)
$(\text{NC})\text{N}(\text{NO}_2)^- + \text{H}^+ \rightarrow (\text{HNC})\text{N}(\text{NO}_2)$	-297.9	RHF 6-31G(+)(d,p)
$(\text{NC})\text{N}(\text{NO}_2)^- + \text{H}^+ \rightarrow (\text{NC})\text{N}(\text{NO}_2\text{H})$	-321.6	RHF 6-31G(+)(d,p)
$(\text{NC})\text{N}(\text{NO}_2\text{H}) + \text{H}^+ \rightarrow (\text{NC})\text{N}(\text{NO}_2\text{H}_2)^+ \rightarrow \text{H}_2\text{O} + \text{NCNNO}^+$	-122.6	RHF 6-31G(+)(d,p)
$(\text{NC})\text{N}(\text{NO}_2\text{H}) + \text{H}^+ \rightarrow \text{H}_2\text{O} + \text{N}_2\text{O} + \text{CN}^+$	28.2	RHF 6-31G(+)(d,p)
$(\text{NC})\text{NH}(\text{NO}_2) + \text{H}^+ \rightarrow \text{H}_2\text{O} + \text{N}_2\text{O} + \text{CN}^+$	14.4	RHF 6-31G(+)(d,p)
$(\text{HNC})\text{N}(\text{NO}_2) + \text{H}^+ \rightarrow \text{H}_2\text{O} + \text{N}_2\text{O} + \text{CN}^+$	4.5	RHF 6-31G(+)(d,p)
$(\text{NC})\text{N}(\text{NO}_2\text{H}) + \text{H}^+ \rightarrow (\text{NC})\text{NH}(\text{NO}_2\text{H})^+$	-148.1	RHF 6-31G(+)(d,p)
$(\text{NC})\text{N}(\text{NO}_2\text{H}) + \text{H}^+ \rightarrow (\text{HNC})\text{N}(\text{NO}_2\text{H})^+$	-166.2	RHF 6-31G(+)(d,p)
$(\text{HNC})\text{N}(\text{NO}_2) + \text{H}^+ \rightarrow (\text{HNC})\text{NH}(\text{NO}_2)^+$	-182.5	RHF 6-31G(+)(d,p)
$(\text{NC})\text{NH}(\text{NO}_2) + \text{H}^+ \rightarrow (\text{HNC})\text{NH}(\text{NO}_2)^+$	-172.6	RHF 6-31G(+)(d,p)
$(\text{HNC})\text{N}(\text{NO}_2) + \text{H}^+ \rightarrow (\text{HNC})\text{N}(\text{NO}_2\text{H})^+$	-189.9	RHF 6-31G(+)(d,p)
$\text{NC-N-CN} + \text{NO}_3^- \rightarrow \text{NC-N-C}(\text{NO}_3)\text{NH}^-$	-5.4	B3-LYP 6-31G(+)(d,p)
$\text{NC-N-C}(\text{NO}_3)\text{NH}^- \rightarrow \text{NC-N-C}(=\text{O})\text{N}(\text{NO}_2)\text{H}^-$	-34.5	B3-LYP 6-31G(+)(d,p)
$\text{NC-N-C}(=\text{O})\text{N}(\text{NO}_2)\text{H}^- + \text{H}^+ \rightarrow \text{HNC-N-C}(=\text{O})\text{N}(\text{NO}_2)\text{H}$	-305.2	B3-LYP 6-31G(+)(d,p)
$\text{HNC-N-C}(=\text{O})\text{N}(\text{NO}_2)\text{H} + \text{H}^+ \rightarrow \text{HNC-NH-C}(=\text{O})\text{N}(\text{NO}_2)\text{H}^+$	-178.0	B3-LYP 6-31G(+)(d,p)

be ~ 1 , 9 and 15 ms, respectively. For the interested reader we provide Supporting Information as a mpg-file that shows hypergolic ignition.

On the basis of a common understanding of how certain energetic materials are known to decompose to stable products, and the similarity in the products we observed here, a suitable

method to identify the nature of at least one of the possible intermediates was carried out as follows. The reaction of ILs with nitric acid can be slowed down using 34 wt % HNO_3 solutions instead of WFNA. This allows for the possibility to trap reaction intermediates by quenching and then suitably identifying their nature. Here, we performed the biuret test using

the method of Lowry⁴⁵ to identify the presence of peptide-like functionality in the reaction intermediate using Cu^{2+} solutions. Confirmation of the presence of such a functionality together with the observed and theoretical evaluations of all the systematically substituted anions studied here would provide strong evidence for the proposed mechanism (see Discussion).

Materials. The following chemicals were synthesized and characterized: 1-butyl-3-methyl-imidazolium azide (>97%), 1-allyl-3-methyl-imidazolium azide (>97%), 1-butyl-3-methyl-imidazolium dicyanamide (>97%), 1-allyl-3-methyl-imidazolium dicyanamide (>97%), 1-propargyl-3-methyl-imidazolium dicyanamide (>97%), 1-methyl-4-amino-1,2,4-triazolium dicyanamide (>97%), 1-(3-butenyl)-3-methyl-imidazolium dicyanamide (>97%), 1-(2-pentynyl)-3-methyl-imidazolium dicyanamide (>97%), 1-methyl-4-amino-1,2,4-triazolium nitrocyanoamide (>97%), 1-allyl-4-amino-1,2,4-triazolium nitrocyanoamide (>97%), and silver nitrocyanoamide (>97%). The characterization data of the above azides is reported elsewhere.⁴⁴ The purities of the above compounds were determined by elemental analysis. Potassium dinitramide (>97%) was kindly supplied by SRI. The following chemicals were purchased from Merck: 1-butyl-3-methyl-imidazolium dicyanamide (>99%), 1-butyl-1-methylpyrrolidinium dicyanamide (>99%), and n-butyl-3-methylpyridinium dicyanamide (>99%). 1-ethyl-3-methyl-imidazolium dicyanamide (>98%) was purchased from Fluka. Sodium azide (>99.5%), sodium dicyanamide (>96%), and silver cyanate (>99%) were purchased from Sigma Aldrich, and white fuming nitric acid (>99.5%) was purchased from Fluka. All chemicals purchased were used without further purification.

Ab Initio Calculations. To predict the proton affinities and reaction enthalpies involved in this study, ab initio calculations were carried out on the Gaussian 03 suite of programs.⁴⁶ Molecular geometries were preoptimized at the Hartree–Fock 3-21G level of theory, and vibrational frequencies were calculated to confirm that a (local) energy minimum had been reached. Subsequent optimization, energy, and vibrational frequency calculations were performed at Hartree–Fock 6-31+G(d,p) level or density functional theory (DFT) level with the hybrid functional, B3LYP 6-31+G(d,p), and these vibrational frequencies confirmed that the optimized structures were minima on the potential energy surface. The HF zero-point vibrational energies (ZPVE) were scaled by 0.9153 and the DFT zero-point energies were scaled by 0.9806.⁴⁷ The corrected zero-point energies were added to the stationary point energies. No thermal corrections were made to determine the reaction enthalpies at 298 K, and the values reported here are at 0 K. Reaction enthalpies at 0 K were calculated by subtracting the sum of the heats of formation of the reactants from the sum of the heats of formation of the products. Table 1 shows the predicted proton affinities and reaction enthalpies at 0 K of the various reaction steps considered here. A more detailed ab initio study will be the subject of a future publication.

Results

FTIR absorption spectra of the gas-phase species evolved when ILs react with white fuming nitric acid can be seen in Figures 3–6. In Figure 3, product peaks in the reaction of 1-butyl-3-methyl-imidazolium azide with WFNA, which does not ignite, are shown. To improve the signal-to-noise ratio, an average of 11 scans (obtained in the time range 270–620 ms) was taken after the spectrometer was triggered. One distinct N_2O and two HN_3 peaks are detected with origins at 2223.5, 2139.6, and 1149.4 cm^{-1} , respectively. The expected HN_3 absorption peak at $\sim 3336 \text{ cm}^{-1}$ is too weak to be discerned

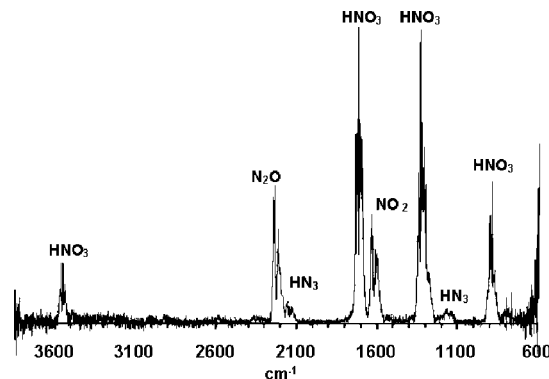


Figure 3. IR product spectrum of 1-butyl-3-methyl-imidazolium (BMIM) azide reacting with WFNA.

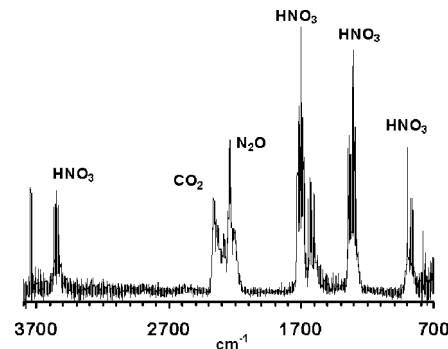


Figure 4. IR product spectrum of BMIM dicyanamide reacting with WFNA.

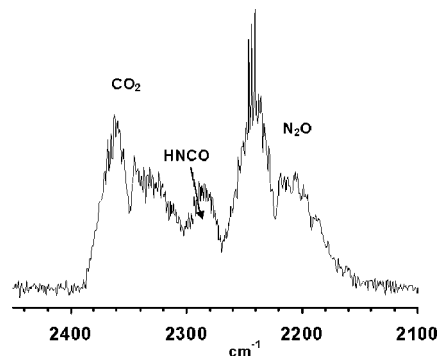


Figure 5. IR product spectrum of BMIM dicyanamide reacting with WFNA. The evolution of CO_2 , N_2O , and HNCO is shown here.

from the recorded spectral noise.⁴⁸ All other peaks in the spectrum have been assigned to gaseous HNO_3 and NO_2 . When 1-butyl-3-methyl-imidazolium dicyanamide is reacted with WFNA, both CO_2 (origin = 2348.4 cm^{-1}) and N_2O (origin = 2222.6 cm^{-1}) are evolved before ignition, as seen in Figure 4. Upon closer inspection, a peak is seen which appears in between the CO_2 and N_2O peaks (Figure 5). Figure 6 shows the result of subtracting the N_2O and CO_2 contributions to the spectrum in Figure 5, after having normalized the N_2O peak data with Figure 3 and the CO_2 peak with an ambient spectrum. The residual absorption feature has an origin at approximately 2269 cm^{-1} and is identified as isocyanic acid (HNCO). Absent in the spectra of the preignition vapor phase are any other gaseous combustion products; HCN , HONO , NO , and CO . Absorptions by H_2O , which is possible according to our mechanism as discussed later, can be observed in Figure 4 near ~ 1600 and $\sim 3750 \text{ cm}^{-1}$.

The time profile of the isocyanic acid product tracks with the N_2O and CO_2 products, as seen in Figure 7. Upon systematic

substitution of cyano groups by nitro groups on the dicyanamide anion, comparison of the reactivity of sodium dicyanamide ($\text{NaN}(\text{CN})_2$), silver nitrocyanamide ($\text{AgN}(\text{CN})\text{NO}_2$), and potassium dinitramide ($\text{KN}(\text{NO}_2)_2$) with WFNA was carried out. Sodium dicyanamide reacts violently with WFNA, producing CO_2 , N_2O , and HNCO (see Figure 8) before igniting ($\text{ID} \approx 825$ ms), as did all the heterocyclic dicyanamide ILs with their own characteristic ID times which we report elsewhere.⁴⁹ The observed gas-phase species time profiles in the reaction of $\text{NaN}(\text{CN})_2$ salt and WFNA were similar to that in Figure 7. The nitrocyanamide salt does not ignite and FTIR measurements showed that the nitrocyanamide anion did not react to produce any detectable gaseous products (in fact, only the initial HNO_3 and NO_2 constituents of the WFNA are observed). The dinitramide salt reacted slowly without ignition to evolve N_2O .

In comparing the spectra of all dicyanamides, only the CO_2 , N_2O , and isocyanic acid are common products. The observed $\text{CO}_2/\text{N}_2\text{O}$ product signal ratio in IL-dicyanamide reactions with WFNA were similar to that in sodium dicyanamide's reaction, suggesting minimal influence of the cation on the reaction temperature for which the data was collected. However, for both 1-propargyl-3-methyl-imidazolium dicyanamide and 1-allyl-3-methyl-imidazolium dicyanamide, a new peak emerges which is centered at 1800 cm^{-1} (Figure 9). The appearance of this species occurs only just before ignition (within 15 to 43 msec) and could possibly be a fragment product coming from reaction at the unsaturated functional group of the cation.

The main findings of the biuret reaction test were as follows. When the reaction of $\text{NaN}(\text{CN})_2$ (90 mg) with 34 wt % HNO_3 (1 drop) was quenched after a minute using excess 2% KOH solution, a cloudy deep purple-pink complex resulted on the addition of 2–4 drops of 1% CuSO_4 solution, which turned cloudy pink within a few minutes and remained stable for many hours. A similar result was also obtained for 1-butyl-3-methyl-imidazolium dicyanamide/34 wt % HNO_3 system. Blank runs in which no acid was added but the same amount of KOH was used produced no change in the coloration upon Cu^{2+} addition. These solutions remained light blue. The pink color change for the dicyanamide/ HNO_3 systems indicates a positive biuret test in which the reaction intermediate (which has a biuret or peptide-like functionality) reacts with the $\text{Cu}(\text{II})$ ions to form a $\text{Cu}(\text{I})$ -coordination complex. When the same tests were performed for the HNO_3 reaction with 1-methyl-4-amino-1,2,4-triazolium nitrocyanamide and 1-allyl-4-amino-1,2,4-triazolium nitrocyanamide, no pink coloration was observed.

Discussion

All of the azides when treated with WFNA or inhibited red fuming nitric acid (IRFNA) failed to ignite. Displacement by the weaker acid on excess addition of nitric acid leads to evolution of HN_3 into the gas phase. The observed N_2O (with coproduct N_2) arises as a result of decomposition of the NON_3 intermediate⁵⁰ formed in the condensed-phase interaction of N_3^- with NO^+ . The source of NO^+ is the autoionization reaction, ($\text{N}_2\text{O}_4 \leftrightarrow \text{NO}^+ + \text{NO}_3^-$) which is possible since small amounts of NO_2 can be present in WFNA and up to $\sim 14\%$ is dissolved in WFNA to form the IRFNA. The initial heat release from the N_3^- ion decomposition to form N_2 and N_2O is not sufficient in our tests to further decompose the heterocyclic counteranion to cause ignition, even when (partial) oxidation of the cation may concurrently contribute to the heat release.⁴⁴ CAUTION: The product, hydrazoic acid (HN_3) is a highly toxic pungent smelling compound whose vapor can cause violent headaches. HN_3 acts as a noncumulative poison. A low but potentially fatal

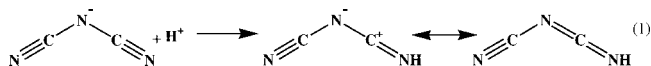
dosage of NO_2 by inhalation can lead to lung edema. Low concentration (4 ppm) exposures can anesthetize the nose, thus creating a potential for overexposure. It must also be emphasized that WFNA and IRFNA are violently reactive, hazardous, and toxic materials and only small quantities should be used under well-ventilated conditions with carefully planned safety protocols and protective equipment in place. The present experimental setup of Figure 1 (details not shown) allowed for the proper containment and disposal of all the materials tested and their reaction products.

The identification of HNCO by FTIR and the elimination of competing possibilities is now addressed. Because the peak at $\sim 2269\text{ cm}^{-1}$ is also present when sodium dicyanamide salt is reacted with WFNA, it cannot be a product resulting from reaction with the imidazolium cation. This is further evidenced by the lack of high frequency hydrogen stretching modes expected from hydrocarbon products of reaction with the imidazolium cation, and which are also absent for the azide IL with the same cation (Figure 3). Known cyanogen ($\text{N}\equiv\text{C}-\text{C}\equiv\text{N}$)⁵¹ absorption features could not be matched with the data of Figure 6, and the presence of cyanamide ($\text{H}_2\text{NC}\equiv\text{N}$)⁵² is also ruled out based on the fact that there was no evidence for absorption at 1055 cm^{-1} due to the $\nu_4(\text{N}-\text{CN})$ symmetric stretching mode.^{52,53} Instead, a match of the data was found with the spectrum for isocyanic acid (HNCO).^{54,55} According to Herzberg and Reid,⁵⁴ the $\nu_2(\text{N}=\text{C}=\text{O})$ asymmetric stretching mode centered at $\sim 2274\text{ cm}^{-1}$ (and more recently reported by Steiner and co-workers to be at 2268.9 cm^{-1} ⁵⁶ and Fisher and co-workers to be at 2259 cm^{-1} ⁵⁷) can be identified here to be responsible for the observed strong absorption. HNCO also has two smaller peaks centered at ~ 797 and $\sim 3531\text{ cm}^{-1}$ with 31% and 24% of the peak height at 2274 cm^{-1} . Even with poor signal-to-noise ratio in the 800 cm^{-1} region, the former peak for the $\nu_4(\text{H}-\text{N}=\text{CO})$ bend is just discernible in Figure 4, while the latter peak for $\nu_1(\text{H}-\text{NCO})$ stretch remains apparently concealed by the large HNO_3 peak at around 3550 cm^{-1} . The other three bands, ν_3 , ν_5 , and ν_6 , respectively at 1322, 577, and 656 cm^{-1} are too weak, and in any case, the former is masked by the strong HNO_3 peaks while the latter two are in the detection cutoff vicinity of the present detector. Also, the observed 2269 cm^{-1} feature is not due to the ν_2 stretching features of fulminic acid (HCNO), which is reported to be at $\sim 2196\text{ cm}^{-1}$ (and thus to the red of the N_2O absorption),^{58,59} or of cyanic acid (HOCN) reported to be at $\sim 2302\text{ cm}^{-1}$ ⁶⁰ since its corresponding $\nu_4(\text{HO}-\text{CN})$ stretching absorption at $\sim 1082\text{ cm}^{-1}$ is not seen in our data.⁶¹ Both HCNO and HOCN are higher energy isomers of HNCO and are not expected to be in any significant amounts in the gas phase.⁶²

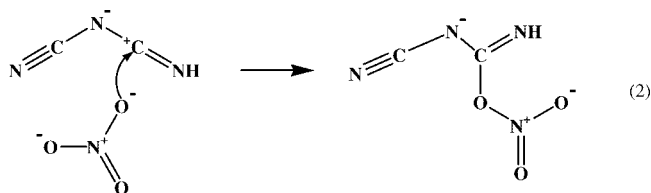
It is well-known that nitriles can undergo acid catalyzed hydration reactions.⁶³ Because the protonated form is much more receptive to nucleophiles at the nitrile carbon, water adds slowly to the carbon and then rearranges to form an amide. The acid-catalyzed reaction with the dicyanamide anion can occur in a similar fashion, but when reacting with WFNA, the nucleophile is NO_3^- instead of H_2O , and the nitrile functional group is subsequently converted to a $\text{C}(=\text{O})\text{NHNO}_2$ group. Because NO_3^- is a better nucleophile than water,⁶⁴ the rate of addition of NO_3^- to the carbon center is expected to be faster than for water in WFNA conditions.

The details of the proposed mechanism for the reaction of the dicyanamide anion with nitric acid are presented here. The first step is to protonate the dicyanamide anion at the nitrile nitrogen, followed by NO_3^- attack at the electrophilic carbon

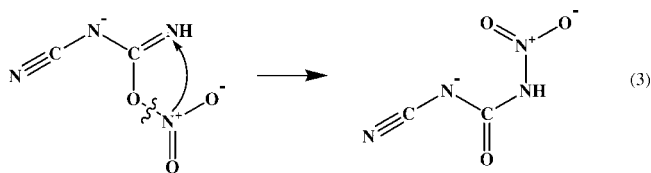
and NO₂ migration to the terminal nitrogen (see Table 1 for calculated energetics):



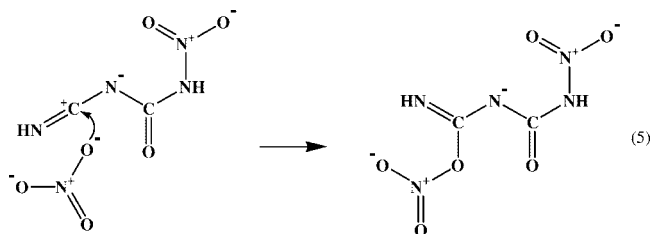
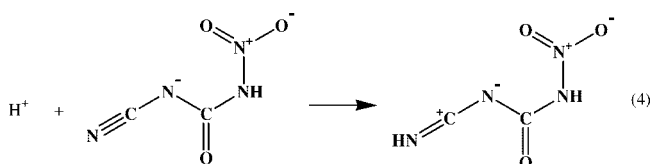
The calculated gas-phase proton affinity of the nitrile nitrogen is about 7.6 kcal mol⁻¹ greater than that for the central nitrogen at the B3-LYP/6-31+G(d,p) level of theory. This is consistent with previous experimental observations for the preferred protonation at the nitrile nitrogen in the topochemical solid-state transformation of ammonium dicyanamide into dicyandiamide.⁶⁵ The reduced electron density at the imine-carbon makes it susceptible to nucleophilic attack by NO₃⁻, which is calculated to be exothermic by 5.4 kcal mol⁻¹:



Subsequent 1,3-shift of NO₂ to the terminal nitrogen, can lead to the formation of a C=O double bond and reaction 3 is calculated to be exothermic by 34.5 kcal mol⁻¹:

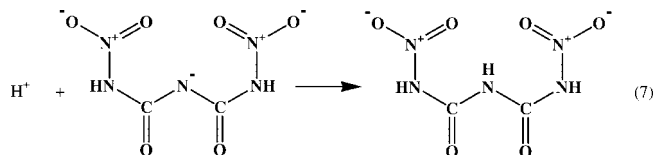
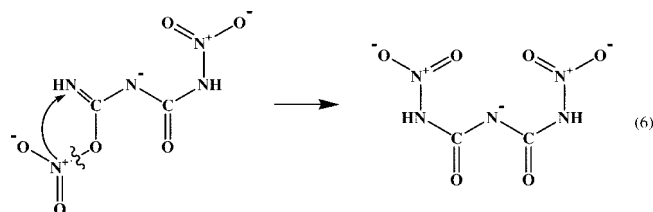


The above reaction sequence is similarly possible starting at the other nitrile nitrogen to form the dinitrobiuret (DNB) anion:



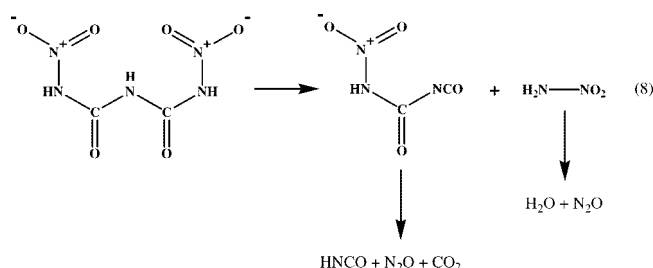
Because of the number of atoms in these molecules, the thermochemistry was not calculated for these species. However, the enthalpies of reactions 4–6 are likely to be comparable to reactions 1–3. Final protonation at the central nitrogen will produce DNB:

The results of the present calculations tabulated in Table 1 show that the crucial NO₃⁻ addition step of reaction 3 and subsequent rearrangement to form the amide linkage of reaction 4 are



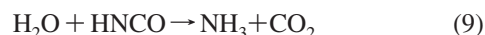
energetically favorable as are many of the protonation steps. Other, alternate and energetically possible mechanistic routes for DNB formation, particularly in nitric acid solutions, could involve either attack by the weaker H₂O nucleophile at the imine-carbon of NCN=C=NH followed by NO₂⁺ addition and subsequent deprotonation to form nitrobiuret (NB),⁶⁶ or the NCN=C=NH intermediate may first undergo another protonation followed by NO₃⁻ addition/rearrangement reactions to yield the NB. These possibilities and the reaction dynamics of DNB formation and decomposition are currently being studied using ab initio methods to determine reaction enthalpies, barrier heights, transition state properties, etc.

The thermal decomposition of DNB has previously been shown to produce CO₂, N₂O, and HNCO,⁶⁷ the same products that we have observed in this work:



The production of CO₂, N₂O, and HNCO from the derivative intermediate and N₂O and H₂O from the nitramide intermediate in reaction 8 must occur through a multistep process, and the decomposition of these chemically labile species may be acid catalyzed. The proposed dicyanamide/WFNA reaction mechanism is consistent with the lack of any HCN or H₂NCN in our gas-phase FTIR spectra. Observation of only isocyanic acid, HNCO, and not of its higher energy isomers is consistent with their known thermal instabilities above ~100 °C.⁶⁸ Treatment of (NaN(CN)₂) with 34% and 68% HNO₃ solutions both resulted in similar product evolution as seen in Figure 5, which is consistent with DNB formation under concentrated acid conditions. Our positive biuret reaction tests provide strong evidence for a peptide like functionality, -HN(O=C)NHC(=O)NH-, in the reaction intermediate. This supports the stance that it is the reaction of dicyanamide anion that initiates the decomposition of the IL salt, and oxidation of the cation becomes important only later after ignition has occurred in WFNA.

HNCO is known to react in the gas phase with water to form CO₂ and ammonia.^{68,69}



Ammonia can react very rapidly with the nitric acid to form NH₄NO₃ which could be why it was not detected in our FTIR

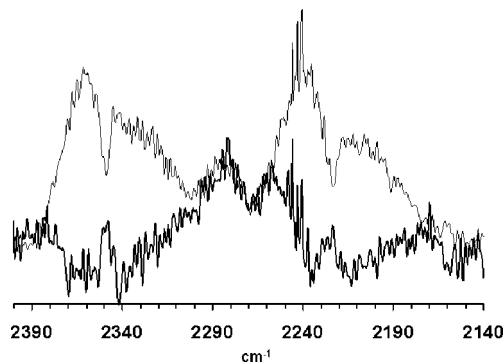


Figure 6. Difference product spectrum of BMIM dicyanamide reacting with WFNA. The dark line is the spectrum of HNCO when the CO_2 and N_2O contributions are subtracted out.

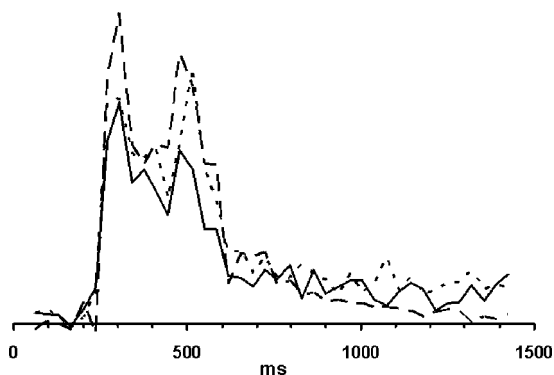


Figure 7. Product time profiles in the reaction of BMIM dicyanamide with WFNA: CO_2 (solid), HNCO (dashed), and N_2O (dotted). Data shown is for case when mixture did not ignite.

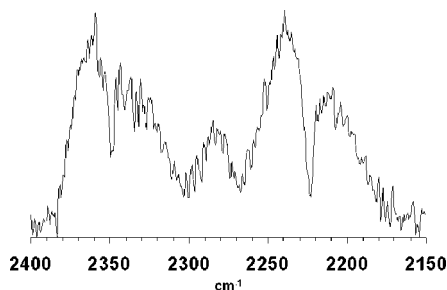
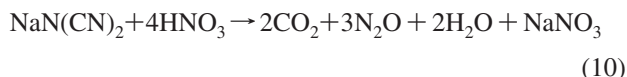


Figure 8. IR product spectrum of sodium dicyanamide reacting with WFNA. Note that the evolution of CO_2 , N_2O , and HNCO is similar to Figure 5.

setup. Here, corresponding hydrolytic decomposition in the condensed phase, $\text{H}_3\text{O}^+ + \text{HNCO} \rightarrow \text{NH}_4^+ + \text{CO}_2$, would also be consistent with lack of NH_3 gas-phase signals. Thermal decomposition of NH_4NO_3 is known to be accelerated in strong mineral acids and can lead to additional N_2O formation.⁷⁰ Thus, in the case if HNCO reacts to completion in nitric acid solution, the maximum $[\text{CO}_2]/[\text{N}_2\text{O}]$ ratio possible would be 2/3 as shown below:



Gas-phase detection of HNCO in our drop-test experiments would suggest that the observed $\text{CO}_2/\text{N}_2\text{O}$ signal represents a ratio less than 2/3 during the preignition phase and that possibly further reactions of HNCO and/or other vapors from DNB decomposition lead to the gas-phase ignition of the IL fuels and salts studied here as seen in Figure 2c.^{67,71} The difference

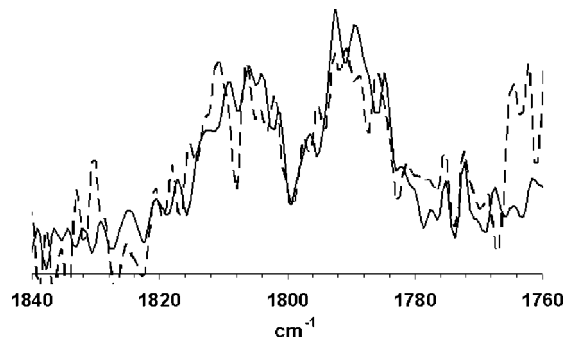


Figure 9. IR product spectrum of 1-propargyl-3-methyl imidazolium dicyanamide (solid) and 1-allyl-3-methyl-imidazolium dicyanamide (dashed) reacting with WFNA showing possible unsaturated species peak near 1800 cm^{-1} .

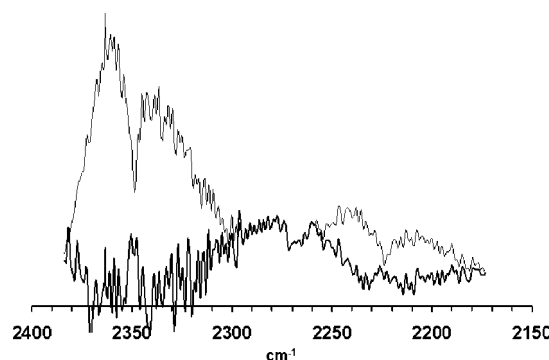
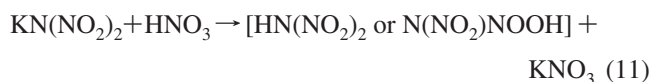
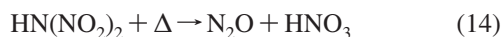


Figure 10. IR product spectrum of silver cyanate (AgOCN) reacting with WFNA. Note that the evolution of CO_2 and HNCO is similar to that shown in Figure 5, but N_2O production is less. The dark line is the difference spectrum for HNCO.

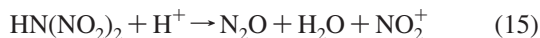
spectrum in Figure 6 shows the infrared spectrum of HNCO formed in the reaction of WFNA with 1-butyl-3-methyl-imidazolium dicyanamide, Figure 8 shows product spectrum for WFNA with sodium dicyanamide, and Figure 10 shows the difference spectrum when silver cyanate (AgOCN) is reacted with WFNA. The ratio of intensities of $\text{CO}_2/\text{N}_2\text{O}$ in Figure 10 is different from that in Figure 8 indicating a different reaction stoichiometry than for the dicyanamides, with less N_2O formation since its source can only be from hydrolysis of HNCO formed in the exothermic condensed phase reaction of AgOCN with nitric acid. Observation of only HNCO in the gas phase would be consistent with its known stability relative to HOCN or HCNO . The band shape at 2271 cm^{-1} in Figure 10 is similar to that in Figure 8, further confirming that indeed HNCO is released in the dicyanamide/nitric acid systems. No visible flames were observed in AgOCN/WFNA tests.

The effect of nitro-substitution for cyano groups on the dicyanamide anion reactivity with WFNA was investigated by reacting WFNA with silver nitrocyanamide or potassium dinitramide. Significant gaseous products were observed for the dinitramide salt, in which N_2O production results from acid catalyzed (and/or thermal) decomposition of the dinitramic acid⁷² without ignition:





The ab initio calculations indicate that both protonation of the central nitrogen followed by a second protonation on the nitro-oxygen or double protonation on the nitro-oxygen can cause the structure to dissociate to N_2O , H_2O , and NO_2^+ .⁷³ ΔH for this reaction is $-205.5 \text{ kcal mol}^{-1}$.



Silver nitrocyanoamide, 1-methyl-4-amino-1,2,4-triazolium nitrocyanoamide, and 1-allyl-4-amino-1,2,4-triazolium nitrocyanoamide failed to ignite in our acid drop tests. From Table 1, the lowest energy gas-phase structure for the protonation of the nitrocyanoamide anion is on the nitro-oxygen. If this species is subsequently protonated at the central nitrogen, analogous to the dinitramide decomposition, the products would be H_2O , N_2O , and CN^+ :



However, the energetics of forming CN^+ versus NO_2^+ is much less favorable, and reaction 16 is higher in energy than reaction 15 by at least $210 \text{ kcal mol}^{-1}$, which is likely why there is no N_2O evolution upon reaction of HNO_3 with nitrocyanoamide. In previous work on decomposition of nitrocyanoamide in strong mineral acids,⁶⁶ no N_2O or any other gaseous products were seen, consistent with our present observations. This suggests that unlike in the above dinitramide case, where double protonation can lead to exothermic decomposition to give N_2O via reaction 15, here this step does not compete with protonation at the $-\text{CN}$ site. Previously the mechanism for nitrocyanoamide/acid reaction in which protonation at the nitrile nitrogen occurs followed by nucleophilic attack by H_2O at the carbon and subsequent OH migration to form nitrourea (NU) has been proposed.⁶⁶ Nitrourea would remain in the condensed phase. Perhaps the amount of heat generated upon formation of nitrourea is insufficient to promote higher energy reactions and cause either gas evolution (i.e., N_2O) or ignition. Also, the decomposition of NU or further nitration of NU to give dinitrourea (DNU) must both be slow in our drop tests, since DNU is thermally unstable and should also give gaseous N_2O and CO_2 .

The allyl-, propargyl-, and (3-butenyl)- functionalized methyl-imidazolium dicyanamides display very violent ignitions with WFNA, giving off a white flash, rather than a typically yellow flash, indicating a hotter temperature in the ignition. Evidence of pyrolytic decomposition of the cation was also seen in the high-speed videos in which copious production of sootlike matter upon ignition was detected. Initially, these functional groups were introduced to try and trigger the fuel-rich cation to ignite. However, now that the dicyanoamide anion is the trigger for the ignition, the cation can be tailored for the best overall properties of the ionic liquid. For example, the allyl-, propargyl-, and (3-butenyl)- functionalized methyl-imidazolium dicyanamides are liquids at room temperature (rt), while the (2-pentynyl)- analogue is a solid at rt. The anion reacts to give off significant heat in the fast formation of CO_2 and N_2O , which causes subsequent decomposition of the cation. The appearance of an unsaturated $\text{C}=\text{C}$ stretch might indicate that the addition of unsaturated functional groups causes the production of smaller, unsaturated hydrocarbons in the gas phase which can greatly aid in combustion once the temperature threshold is reached (evidence for this was seen as secondary ignition flashes in the high-speed video recordings). This peak is only seen in the allyl- and propargyl-functionalized methyl-imidazolium

dicyanoamide species, and not in the corresponding (3-butenyl)-system, and thus more work is needed to uncover the details of how substitution affects the decomposition/oxidation mechanisms of the heterocyclic cation.

Conclusions

The hypergolic ignition of dicyanoamide ionic liquids upon reaction with fuming nitric acid has been demonstrated, and it has been shown that the anion reaction is responsible for initiating the ignition. The evolution of CO_2 , N_2O , and HNCO during preignition indicates a complex reaction mechanism, perhaps through dinitrobiuret and nitramide intermediates. Evidence for the former was confirmed in the biuret reaction test which was only positive for the dicyanoamide reactions and not with any of the other anions studied here. In this work we have shown that the initial reactivity of the anions, $^-\text{N}(\text{CN})_2$, $^-\text{NNO}_2(\text{CN})$, and $^-\text{N}(\text{NO}_2)_2$, with WFNA varies dramatically with NO_2 substitution. Similarly, it may also be possible to affect the cation reactivity by suitable chemical substitutions, so as to tailor its oxidation rate. Further spectroscopic probing of products and intermediates during the preignition and ignition phases and additional ab initio calculations will be valuable in providing mechanistic insight on how IL-dicyanamides undergo combustion when treated with WFNA and IRFNA.

Acknowledgment. Funding for this work was provided by the Air Force Office of Scientific Research under Contract No. FA9300-06-C-0023 with the Air Force Research Laboratory, Edwards AFB, CA 93524.

Supporting Information Available: Video (one mpg-file) showing hypergolic ignition of 1-propargyl-3-methyl-imidazolium dicyanoamide in WFNA. This material is available free of charge via the Internet at <http://pubs.acs.org>.

References and Notes

- (1) See for example: Smiglak, M.; Metelen, A.; Rogers, R. D. *Acc. Chem. Res.* **2007**, *40*, 1182, and references therein.
- (2) Kelkar, M. S.; Maginn, E. J. *J. Phys. Chem. B* **2007**, *111*, 9424.
- (3) Deetlefs, M.; Seddon, K. R.; Shara, M. *Phys. Chem. Chem. Phys.* **2006**, *8*, 642.
- (4) Eike, D. M.; Brennecke, J. F.; Maginn, E. J. *Green Chem.* **2003**, *5*, 323.
- (5) Katritzky, A. R.; Jain, R.; Lomaka, A.; Petrukhin, R.; Karelson, M.; Visser, A. E.; Rogers, R. D. *J. Chem. Inf. Comput. Sci.* **2002**, *42*, 225.
- (6) Zhang, S.; Ning, S.; Xuezhong, H.; Xingmei, L.; Xianping, Z. *J. Phys. Chem. Ref. Data* **2006**, *35*, 1475.
- (7) Gutowski, K. E.; Holbrey, J. D.; Rogers, R. D.; Dixon, D. A. *J. Phys. Chem. B* **2005**, *109*, 23196.
- (8) Hawkins, T. W. *Ionic Liquids and their Applications: Pathways and Bottlenecks to their Use*; AFOSR Contractors Workshop, 2006, Tuscaloosa, AL.
- (9) Scammells, P. J.; Scott, J. L. D. S. R. *Aust. J. Chem.* **2005**, *58*, 155.
- (10) Rogers, R. D.; Voth, G. A. *Acc. Chem. Res.* **2007**, *41*, 1077. and articles therein on the special issue, "Ionic Liquids"
- (11) Wishart, J. F.; Castner, E. W. *J. Phys. Chem. B* **2007**, *111*, 4369. and articles therein on the special issue, "The Physical Chemistry of Ionic Liquids"
- (12) Macfarlane, D. R.; Meakin, P.; Sun, J.; Amini, N.; Forsyth, M. *J. Phys. Chem. B* **1999**, *103*, 4164.
- (13) Ngo, H. L.; LeCompte, K.; Hargens, L.; McEwen, A. B. *Thermochem. Acta* **2000**, *357*, 97.
- (14) Xie, W.; Xie, R.; Pan, W.-P.; Hunter, D.; Koene, B.; Tan, L.-S.; Vaia, R. *Chem. Mater.* **2002**, *14*, 4837.
- (15) Fredlake, C. P.; Crosthwaite, J. M.; Hert, D. G.; Aki, S. N. V. K.; Brennecke, J. F. *J. Chem. Eng. Data* **2004**, *49*, 954.
- (16) Baranyai, K. J.; Deacon, G. B.; Macfarlane, D. R.; Pringle, J. M.; Scott, J. L. *Aust. J. Chem.* **2004**, *57*, 145.
- (17) Macfarlane, D. R.; Pringle, J. M.; Johansson, K. M.; Forsyth, S. A.; Forsyth, M. *Chem. Commun.* **2006**, 1905.

- (18) Huddleston, J. G.; Visser, A. E.; Reichert, W. M.; Willauer, H. D.; Broker, G. A.; Rogers, R. D. *Green Chem.* **2001**, *3*, 156.
- (19) Holbrey, J. D.; Seddon, K. R. *J. Chem. Soc., Dalton Trans.* **1999**, 2133.
- (20) Earle, M. J.; Esperanca, J. M. S. S.; Gilea, M. A.; Lopes, J. N. C.; Rebelo, L. P. N.; Magee, J. W.; Seddon, K. R.; Widegren, J. A. *Nature* **2006**, *439*, 831.
- (21) Armstrong, J. P.; Hurst, C.; Jones, R. G.; Licence, P.; Lovelock, K. R. J.; Satterley, C. J.; Villar-Garcia, I. J. *Phys. Chem. Chem. Phys.* **2007**, *9*, 982.
- (22) Leal, J. P.; Esperanca, J. M. S. S.; Minas de Piedade, M. E.; Lopes, J. N. C.; Rebelo, L. P. N.; Seddon, K. R. *J. Phys. Chem. A* **2007**, *111*, 6176.
- (23) Strasser, D.; Goulay, F.; Kelkar, M. S.; Maginn, E. J.; Leone, S. R. *J. Phys. Chem. A* **2007**, *111*, 3191.
- (24) Emel'yanenko, V. N.; Verevkin, S. P.; Heintz, A. *J. Am. Chem. Soc.* **2007**, *129*, 3931.
- (25) Zaitsau, D. H.; Kabo, G. J.; Strechan, A. A.; Paulechka, Y. U.; Tserich, A.; Verevkin, S. P.; Heintz, A. *J. Phys. Chem. A* **2006**, *110*, 7303.
- (26) Gutowski, K. E.; Rogers, R. D.; Dixon, D. A. *J. Phys. Chem. A* **2006**, *110*, 11890.
- (27) Sengupta, D.; Raman, S. *Propellants Explos. Pyrotech.* **2007**, *32*, 338.
- (28) Sutton, G. P. *J. Propul. Power* **2003**, *6*, 978.
- (29) Sutton, G. P. *J. Propul. Power* **2003**, *6*, 1008.
- (30) Catoire, L.; Chaumeix, N.; Paillard, C. *J. Propul. Power* **2004**, *20*, 87.
- (31) Frank, I.; Hammer, A.; Klapotke, T. M.; Nonnenberg, C. *Propellants Explos. Pyrotech.* **2005**, *30*, 44.
- (32) McQuaid, M. J.; Ishikawa, Y. *J. Phys. Chem. A* **2006**, *110*, 6129.
- (33) Osmond, A.; Catoire, L.; Klapotke, T. M.; Vaghjiani, G. L.; Swihart, M. T. *Propellants Explos. Pyrotech.* **2008**, *33*, 209.
- (34) Seamans, T. F.; Vanpee, M.; Agosta, V. D. *AIAA J.* **1967**, *5*, 1616.
- (35) Nonnenberg, C.; Frank, I.; Klapotke, T. M. *Angew. Chem., Int. Ed.* **2004**, *43*, 4586.
- (36) Catoire, L.; Chaumeix, N.; Pichon, S.; Paillard, C. *J. Propul. Power* **2006**, *22*, 120.
- (37) Hampton, C. S.; Smith, J. E. *The Importance of Carbon, Nitrogen, and Oxygen Atomic Ratios on the Combustion of Hypergolic Bipropellants*; Paper AIAA 2005-740, 43rd AIAA Aerospace Sciences Meeting and Exhibit, Reno, NV, Copyright 2005 by the American Institute of Aeronautics and Astronautics, Inc.
- (38) Daimon, W.; Tanaka, M.; Kimura, I. *Proceedings on the 20th Symposium on Combustion*; Pittsburgh, PA, 1984; pp 2065–2071.
- (39) de Bonn, O.; Hammerl, A.; Klapotke, T. M.; Mayer, P.; Piotrowski, H.; Zewen, H. *Z. Anorg. Allg. Chem.* **2001**, *627*, 2011.
- (40) Klapotke, T. M.; Rienäcker, C. M.; Zewen, H. *Z. Anorg. Allg. Chem.* **2002**, *628*.
- (41) Patil, D. G.; Jain, R.; Brill, T. B. *Propellants Explos. Pyrotech.* **1992**, *17*, 260.
- (42) Tuazon, E. C.; Carter, W. P. L.; Brown, R. V.; Winer, A. M.; Pitts, J. M. *J. Phys. Chem.* **1983**, *87*, 1600.
- (43) Alfano, A.; Mills, J. D.; Vaghjiani, G. L. *Rev. Sci. Instrum.* **2006**, *77*, 45109.
- (44) Schneider, S.; Hawkins, T. W.; Rosander, M.; Mills, J. D.; Vaghjiani, G. L.; Chambreau, S. D. *Z. Inorg. Chem.* **2008**, *47*, 6082.
- (45) Lowry, O. H.; Rosebrough, N. J.; Farr, A. L.; Randall, R. J. *J. Biol. Chem.* **1951**, *193*, 265.
- (46) Frisch, M. J.; Trucks, G. W.; Schlegel, H. B.; Scuseria, G. E.; Robb, M. A.; Cheeseman, J. R.; Montgomery, J. J. A.; Vreven, T.; Kudin, K. N.; Burant, J. C.; Millam, J. M.; Iyengar, S. S.; Tomasi, J.; Barone, V.; Mennucci, B.; Cossi, M.; Scalmani, G.; Rega, N.; Petersson, G. A.; Nakatsuji, H.; Hada, M.; Ehara, M.; Toyota, K.; Fukuda, R.; Hasegawa, J.; Ishida, M.; Nakajima, T.; Honda, Y.; Kitao, O.; Nakai, H.; Klene, M.; Li, X.; Knox, J. E.; Hratchian, H. P.; Cross, J. B.; Bakken, V.; Adamo, C.; Jaramillo, J.; Gomperts, R.; Stratmann, R. E.; Yazyev, O.; Austin, A. J.; Cammi, R.; Pomelli, C.; Ochterski, J. W.; Ayala, P. Y.; Morokuma, K.; Voth, G. A.; Salvador, P.; Dannenberg, J. J.; Zakrzewski, V. G.; Dapprich, S.; Daniels, A. D.; Strain, M. C.; Farkas, O.; Malick, D. K.; Rabuck, A. D.; Raghavachari, K.; Foresman, J. B.; Ortiz, J. V.; Cui, Q.; Baboul, A. G.; Clifford, S.; Cioslowski, J.; Stefanov, B. B.; Liu, G.; Liashenko, A.; Piskorz, P.; Komaromi, I.; Martin, R. L.; Fox, D. J.; Keith, T.; Al-Laham, M. A.; Peng, C. Y.; Nanayakkara, A.; Challacombe, M.; Gill, P. M. W.; Johnson, B.; Chen, W.; Wong, M. W.; Gonzalez, C.; Pople, J. A. *Gaussian 03*; revision C.02; Gaussian, Inc.: Wallingford, CT, 2004.
- (47) Scott, A. P.; Radom, L. *J. Phys. Chem.* **1996**, *100*, 16502.
- (48) Dows, D. A.; Pimentel, G. C. *J. Chem. Phys.* **1955**, *23*, 1258.
- (49) Hawkins, T. W.; Rosander, M.; Vaghjiani, G. L.; Chambreau, S. D.; Drake, G.; Schneider, S. *Energy Fuels* **2008**, *22*, 2871.
- (50) Lucien, H. W. *J. Am. Chem. Soc.* **1958**, *80*, 4458.
- (51) PNNL Infrared Spectral Library. <http://nwir.pnl.gov/> (accessed Sept 2007).
- (52) Bark, M.; Winnissner, M. *Chem. Phys. Lett.* **1986**, *123*, 382.
- (53) Wagner, G. D. J.; Wagner, E. L. *J. Chem. Phys.* **1960**, *64*, 1480.
- (54) Herzberg, G.; Reid, C. *Discuss. Faraday Soc.* **1950**, *9*, 92.
- (55) Nelson, P. F.; Li, C.-Z.; Ledesma, E. *Energy Fuels* **1996**, *10*, 264.
- (56) Stiner, D. A.; Polo, S. R.; McCubbin, T. K. *J. Mol. Spectrosc.* **1983**, *98*, 453.
- (57) Fischer, G.; Geith, J.; Klapotke, T. M.; Krumm, B. *Z. Naturforsch.* **2002**, *57b*, 19.
- (58) Ferretti, E. L.; Rao, K. N. *J. Mol. Spectrosc.* **1974**, *51*, 97.
- (59) Grubdorff, J.; Temps, W. H. *Ber. Bunsenges. Phys. Chem.* **1997**, *101*, 134.
- (60) Su, H.; Kong, F.; Chen, B.; Huang, M.-B.; Lui, Y. *J. Chem. Phys.* **2000**, *113*, 1885.
- (61) Crowley, J. N.; Sodeau, J. R. *J. Phys. Chem.* **1989**, *93*, 3100.
- (62) Ruscic, B.; Berkowitz, J. *J. Chem. Phys.* **1994**, *100*, 4498.
- (63) Streitwieser, A., Jr.; Heathcock, C. H. *Introduction to Organic Chemistry*, 3rd ed.; Macmillan Publishing Co.: New York, 1985.
- (64) Edwards, J. O. *J. Am. Chem. Soc.* **1954**, *76*, 1540.
- (65) Lotsch, B. V.; Senker, J.; Schnick, W. *Inorg. Chem.* **2004**, *43*, 895.
- (66) Astraf'ev, A. A.; Kuznetsov, L. L. *Russ. J. Org. Chem.* **2002**, *38*, 1252.
- (67) Geith, J.; Holl, G.; Klapotke, T. M.; Weigand, J. *J. Combust. Flame* **2004**, *139*, 358.
- (68) Fisher, G.; Geith, J.; Klapotke, T. M.; Krumm, B. *Z. Naturforsch.* **2002**, *57b*, 19.
- (69) Belson, D. J.; Strachan, A. N. *Chem. Soc. Rev.* **1982**, *11*, 41.
- (70) See for example: Sun, J.; Sun, Z.; Wang, Q.; Ding, H.; Wang, T.; Jiang, C. *J. Hazard. Mater.* **2005**, *127B*, 204, and references therein.
- (71) Geith, J.; Klapotke, T. M. *J. Mol. Struct. (THEOCHEM.)* **2001**, *538*, 29.
- (72) Lobbecke, S.; Keicher, T.; Krause, H.; Pfeil, A. *Solid State Ionics* **1997**, *101*, 945.
- (73) Politzer, P.; Seminario, J. P. *Chem. Phys. Lett.* **1993**, *216*, 348.